Effect of polycarboxylate superplasticizer on hydration and properties of belite ye'elimite ferrite cement paste

A. Barneoud-Chapelier, G. Le Saout, N. Azéma, Y. El Bitouri*

LMGC, IMT Mines Ales, Univ. Montpellier, CNRS, Ales, France

*Corresponding author

Tel.: +33-4-66-78-53-05

E-mail: youssef.elbitouri@mines-ales.fr

Abstract

Belite-Ye'elimite-Ferrite (BYF) cements have received increasing attention in view of their lower CO_2 footprint and their interesting performances. This work deals with the effect of polycarboxylate superplasticizer (SP) on BYF cement paste. It was found that SP dosage must be low in order to avoid destabilization, and thus improve the resistance to bleeding and segregation. Also, the good affinity of polycarboxylate based superplasticizer with cement surface improves the cement particles dispersion and causes a significant diminution of the yield stress during the low activity period. Furthermore, it is shown that SP causes a delay in the early age hydration, inducing a decrease in the compressive strength at early age while it increases them after 90 days.

Keywords: *Belite ye'elimite ferrite cement, admixture , hydration , rheology , cement paste*

1 Introduction

Cement industry is responsible for 8% of global anthropogenic CO_2 emissions [1], mainly due to ordinary Portland cement (OPC) production. In order to reduce them, new binders are developed such as Belite-Ye'elimite-Ferrite (BYF) cements, which production releases up to 30 % less CO_2 [2,3]. They were recently proposed as alternative to OPC considering that their performances tend to be similar [4]. The main raw materials used for making BYF are bauxite, limestone, clay, and gypsum and this leads to a mineralogical composition very different than Portland cement. The three main phases present in BYF clinkers are, in the order of content (cement notation will hereafter be used: C = CaO, S = SiO_2, A = Al_2O_3, F = Fe_2O_3, Š = SO_3, H = H_2O): belite (C_2S), ye'elimite ($C_4A_3Š$) and ferrite (C_4AF). Calcium Sulfo-Aluminate (CSA) clinkers are usually co-grinded with 15 to 25 wt% of calcium sulfate to optimize strength development and volume changes [5].

Previous studies concerning hydration of this cement have shown different hydration steps. First, only ye'elimite and calcium sulfate react [6] during the first day, to form ettringite and aluminum hydroxide [7] (usually poorly crystallized [8–10]) according to the following chemical reaction (1). Then, local concentration of sulfate decreases [11]; they react to form calcium monosulfoaluminate (AFm) according to the second chemical reaction (2). Due to its high reactivity, the conversion rate of ye'elimite can reach 85 % in 6 hours [9].

$$C_4A_3Š + 2\ CŠ + 38\ H \rightarrow C_3A{\bullet}3CŠ\ {\bullet}32H + 2\ AH_3 \quad (1)$$

$$C_4A_3Š + 18\ H \rightarrow C_3A{\bullet}CŠ\ {\bullet}12H + 2\ AH_3 \quad (2)$$

Afterwards, belite begins to hydrate. First, it reacts with aluminum hydroxide originated from ye'elimite hydration to form strätlingite (C_2ASH_8) according to reaction (3). Its

hydration can lead to pH increase [12] which destabilizes strätlingite, usually around 28 days of hydration [9,13,14]; strätlingite reacts with belite to form siliceous hydrogarnet ($C_3AS_{1.3}H_{3.4}$) and C-S-H gel according to reaction (4). Some portlandite can also be formed by the hydration of belite according to reaction (5), but this reaction is more likely to occur in Portland cement or in BYF cements with a particularly high belite content [15].

$$C_2S + AH_3 + 5\,H \rightarrow C_2ASH_8 \quad (3)$$

$$C_2ASH_8 + 2\,C_2S + 2{,}2\,H \rightarrow C_3AS_{1,3}H_{3,4} + 1{,}7\,C_{1,7}SH_4 \quad (4)$$

$$C_2S + (2 - x + y)H \rightarrow C_xSH_y + (2 - y)CH \quad (5)$$

The hydration of ferrite in these cements have not yet well been elucidated, it is suspected to react in the same time as belite, as iron can replace aluminum in strätlingite [11,16]. Iron has also been found in ettringite and aluminum/iron hydroxide [17–20], which suggests its hydration takes place at the same time as ye'elimite.

The hydration of BYF cements remains complex; different experiments and thermodynamic modelling were performed for ye'elimite-containing cements to understand their hydration. Their early hydration – that mainly depends on ye'elimite reactivity – can be tailored by varying the nature [21–23] and amount [5,11,12,21,24,25] of calcium sulfate, or the water-to-binder ratio [12,14,16]. The effect of some retarders on BYF cement hydration was also studied: tartrate, gluconate, borax [26,27] as well as citric acid [28]. Also, the compatibility with polycarboxylate superplasticizer was proved [29,30]; and some studies on the effect of polycarboxylates on CSA cements shown that their dispersion effect was limited in time due to the ettringite precipitation [31,32]. However, the number of studies on the effect of admixtures on this kind of cement remains limited. Therefore, this work deals with the

effect of a polycarboxylate superplasticizer on hydration and rheological properties of BYF cement paste.

Polycarboxylate superplasticizers (PCEs) are widely used in concrete industry since they enable a better workability for concrete, hereby decreasing the placing costs and allowing diminution of water-to-cement ratio. PCEs act by adsorption at the cement particles surface and induce electrostatic repulsion and steric hindrance which enhance the dispersion of cement particles and thus improve the rheology the paste.

Besides their dispersion effect, superplasticizers have an influence on the cement hydration. They strongly interact with ettringite [33] and are known to delay its precipitation [34–36].

The aim of this paper is to investigate the effect of polycarboxylate superplasticizer on microstructure and properties of fresh and hardened BYF cement pastes. Hydration was studied using isothermal calorimetry; phase composition was determined by Rietveld quantitative XRD coupled with TGA. Moreover, consumption of superplasticizer was assessed by TOC measurements and the effect of the SP on rheological and mechanical behavior was also investigated.

2 Experimental section

2.1 Materials

The cement used was obtained by mixing BYF clinker with 10 wt% of natural anhydrite. Its granular properties are given in Table 1, as well as its elemental and mineral composition. The oxide content was determined by XRF, and the mineral content was determined by Rietveld quantitative X-ray powder diffraction.The

amorphous and crystalline non-quantified content (ACn) were determined using an external standard ZnO as detailed in the method section (2.2.3).

Table 1: Granular and chemical properties of the BYF cement used

Granular data		Oxide content (wt%)		Mineral content (wt %)	
Density (g/cm^3)	3.10	CaO	49.2	β-belite	32.8
Blaine surface area (m²/g)	0.40	Al_2O_3	19.3	ye'elimite	24.5
BET surface area (m²/g)	0.77	SiO_2	12.2	ferrite	21.0
Mean grain size (µm)	16.9	SO_3	10.0	gehlenite	1.6
Median grain size (µm)	11.2	Fe_2O_3	7.5	perovskite	1.8
Minimal grain size (µm)	0.04	TiO_2	0.44	anhydrite	9.3
Maximal grain size (µm)	110	MgO	0.29	gypsum	0.4
		K_2O	0.24	calcite	0.3
		MnO	0.1	ACn	7.3
		Na_2O	0.1		
		P_2O_5	0.1		

A commercial polycarboxylate based superplasticizer (Master-Glenium 201, BASF, France) was used. The dry extract was determined in accordance with the European standard EN 480-8. The measured dry extract (19.5 wt%) is the same as that provided by BASF. The characteristics of this superplasticizer are provided in the appendix. The dosage of superplasticizer will hereafter be expressed as mass of dry extract per mass of cement. According to BASF, the recommended range of use of this superplasticizer corresponds to 0.3 – 3 % by total mass of cement, which corresponds to 0.06-0.6% of dry extract. In this study, when SP is used in higher amounts than 0.06 % (i.e. 0.1 % and

0.4 %), the cement paste is strongly destabilized, which means that an excessive bleeding is observed.

Cement pastes were prepared with water to cement weight ratio (w/c) of 0.4 by pouring cement into an aqueous solution containing the appropriate amount of SP (corresponding to time zero of the hydration), while stirring at 500 rpm for 1 min, and then for a further minute at 1000 rpm using a planetary agitator Stuart SS30.

Samples were cured at ambient temperature (23°C± 2°C) and 86 ± 3 % relative humidity on the first day of hydration, and then in tap water. For rheological measurements and interstitial liquid extraction, 5 min before the experiments, the paste was stirred at 1000 rpm for 20 s then at 2000 rpm during 10 s.

2.2 Methods

2.2.1 Isothermal calorimetry

A conduction calorimeter (TAM Air, Thermometric AB, Sweden) operating at 25°C was used to determine the hydration heat flow. About 5 g of paste were weighed into sealed glass flasks and transferred into the calorimeter within 3 min. Results are presented after a normalization by the weight of anhydrous cement.

2.2.2 Thermal analysis

Hydration was stopped by immersing fine powder of the crushed paste for 5 minutes in isopropanol and rinsing twice with diethyl ether. TGA (NETZSCH STA 449F5) was performed using about 80-100 mg of powder at a heating rate of 10°C.min^{-1} under argon between 30 and 950°C, after 10 min of stabilization at 30°C.

2.2.3 X-ray diffraction

Three types of samples were analyzed by X-ray diffraction: anhydrous cement (powder), fresh cement paste (suspension), hardened cement paste (slice). The latter were not analyses quantitatively, as explained in the result part. Patterns were recorded on a Bruker AXS D8 Advanced diffractometer in a θ-θ configuration. X-ray diffraction was performed on anhydrous cement, fresh cement paste and hardened cement paste. Data were collected from 5° to 70° (2θ) during approximatively 1 h (Cu Kα, λ=1.54 Å) during which the sample is rotating to improve the crystallites orientation statistics, for all samples except for fresh cement paste.

Clinker composition was determined thanks to powder X-ray diffraction. An external standard ZnO (G- factor approach) was used to quantify X-ray amorphous and crystalline non-quantified part according to the method presented by Jansen et al. [37], and applied to BYF clinker using X'pert PANalytical software. The structure model used for the Rietveld refinement of the CSA are given in [38]. The mass attenuation coefficients of the samples were calculated using data from X-ray fluorescence analysis (Table 1). The hydrated paste samples were analysed qualitatively

The composition of fresh cement pastes was determined thanks to *in situ* measurements. To this end, the freshly prepared paste was cast into a sample holder, and covered with a Kapton film to avoid evaporation. Data were collected from 5° to 50° (2θ) during 17.5 min for the first 4 hours of hydration. Rietveld refinements were performed on these patterns.

Hardened cement pastes were analysed without crushing them nor stopping their hydration in order to avoid dissolution of ettringite in solvent. Slices (diameter 2 cm)

were sawn under isopropanol with a diamond-coated blade and immediately placed in the diffractometer for XRD pattern acquisition.

2.2.4 Microscopic observations

The fractured cement pastes were observed using Scanning Electron Microscopy (SEM Quanta 200 FEG (FEI)using Back-Scattered Electron mode (BSE).

2.2.5 Superplasticizer consumption

The amount of consumed SP was determined by the depletion method [39]. The interstitial liquid was extracted from the paste by centrifugation (10 min at 10000 rpm), filtered (PTFE 0.45 µm), diluted with milli-Q water and analyzed using a vario TOC cube (Elementar) in total carbon mode, using superplasticizer calibration. To avoid precipitation of hydrates, the measurements were made during the same day as the extraction of interstitial liquid. The result for the reference in which no SP was added was considered to correspond to the amount of inorganic carbon in all samples.

2.2.6 Rheological behavior

Rheological measurements were carried out using an experimental AR 2000ex rheometer from TA Instruments, equipped with parallel-plate geometry covered with sand paper. The measurement procedure consists of a pre-shear phase (during 80 s at 100 s^{-1}) followed by shear rate sweep (from 100 s^{-1} to 0.1 s^{-1}). Due to the complexity of obtaining the steady state flow, for each shear rate, the shear stress was measured at a similar equilibrium time of 20 s for all cement pastes. The dynamic yield stress was determined by extrapolating the Herschel-Bulkley model. All measurements were performed on cement pastes hydrated for 40 min, which corresponds to a low heat activity period.

2.2.7 Compressive strength

Compressive strengths were measured on 20 x 20 x 20 mm cubes of cement pastes prepared in plastic 3D-printed molds. The compressive strength tests were performed mechanical using testing machine (3R-RP40) with force control. The load was applied at a uniform rate of0.1 MPa/s. The specimens were testedat 1, 7, 90 and 180 days of hydration.

Table 2 summarizes all the performed tests and the used mixtures.

Table 2 : The performed tests and the used mixtures

%SP	time of hydration	isothermal calorimetry	In-situ XRD	SEM	TOC	rheology	TGA	XRD	compressive strength
0 %, 0.05 %	0 - 300 min	x	x						
	40 min				x	x			
	5 h			x					
	1, 7, 28, 90 days						x	x	x
0.025 %	1, 7, 28, 90 days								x
0.015 % 0.025 % 0.04 % 0.06 %	40 min	x			x	x			

3 Results and discussion

3.1 Effect of SP during the early age

3.1.1 Early age hydration of the BYF cement without admixture

Fig 1 (top) shows the variation of the phase composition and the heat flow with hydration time during the first four hours of hydration.

Due to the introduction of the sample into the calorimeter, the heat flow signal is disturbed at the beginning of the measurement. The wetting of the cement grains and first dissolution of the first anhydrous species is usually exothermic, leading to a first hydration peak that could not be measured. Yet, its existence is confirmed by the signal rapidly increasing and then decreasing before the first hour of hydration, thereby showing the end of the first phase of hydration and beginning of a low heat activity period. This first period corresponds to the first dissolution of ye'elimite and anhydrite, the latter immediately forming some gypsum, probably due to a local small quantity of other ions than Ca^{2+} and SO_4^{2-} in the interstitial solution. Also, precipitation of ettringite according to (1) seems to start immediately. The gypsum hereby formed has a higher kinetics of dissolution than anhydrite, and, once formed, it quickly dissolves to become the sulfate source consumed by ettringite formation.

After a quick period where the heat flow decreases, at 1 hour of hydration, a slight acceleration in the dissolution of anhydrite and ye'elimite takes place, in accordance with stronger precipitation of ettringite. After 2 hours of hydration, the most intense heat flow peak is observed. It corresponds to even stronger dissolution of ye'elimite, leading not only to the formation of ettringite but also to the first precipitation of calcium monosulfoaluminate (AFm) according to (2). The width of the XRD peaks of the latter (not shown) suggests it is poorly crystallized. At the end of this third peak, the dissolution of anhydrous phases seems to decelerate.

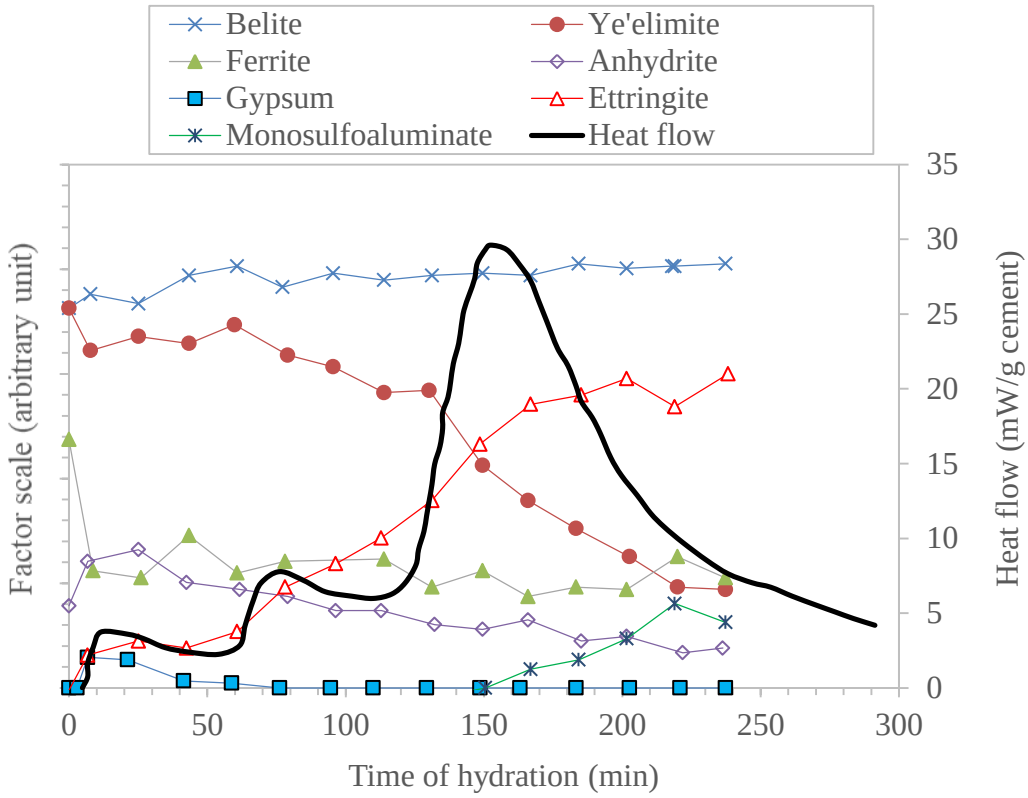

198

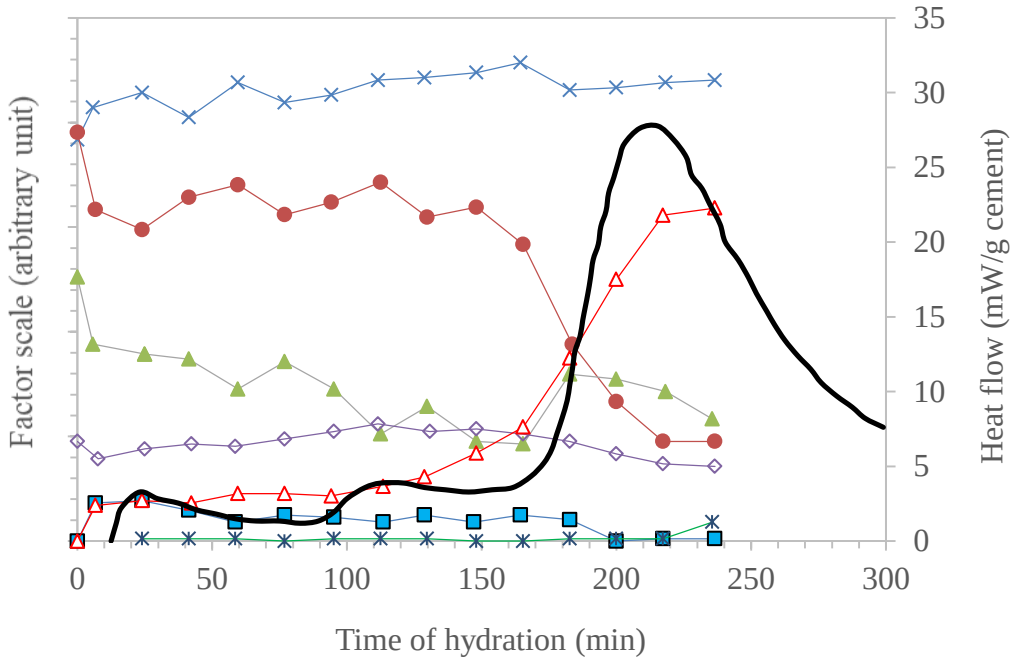

199

200 **Fig 1: Phase composition and heat flow of the cement paste containing (top) no SP and**

201 **(bottom) 0.05 % SP, measured by in-situ RQXRD coupled with isothermal calorimetry.**

3.1.2 Effect of polycarboxylate superplasticizer

The results of isothermal calorimetry of the cement paste without SP and with a dosage of 0.05 % are shown respectively in Fig 1 (bottom) and Fig 2. This SP dosage does not destabilize the cement paste. By comparing these results, it appears that the hydration is delayed when SP is added. Also, with 0.05 % SP, the main peak seems to be a bit larger, which can be due to a slower AFm precipitation, that is observed in Fig 1 and can be hypothesized for longer hydration times.

The delay in the hydration was quantified by measuring the time of hydration at which the calorimetry heat flow increased, corresponding to the beginning of the two detectable peaks (second and third, the first being difficult to measure as previously mentioned). This was measured for increasing amounts of SP and is presented in Fig 2. As shown in this figure, increasing superplasticizer dosage leads to more retarding effect. Especially, the addition of increasing amounts of SP seems to retard the second peak of hydration, when ettringite precipitates massively. The same trends were observed by Su et al. [30] with four superplasticizers on belite rich calcium sulfoaluminate cements. Moreover, after approximately one day of hydration, the cumulated heat is equivalent for all systems.

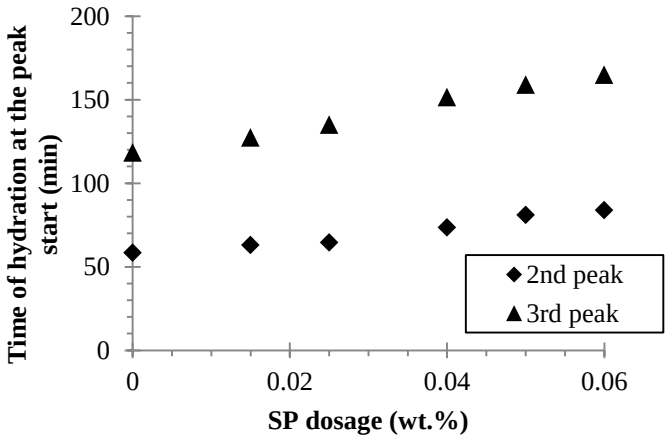

Fig 2: Time of hydration of the cement paste at the beginning of the two main calorimetric peaks for different SP dosages

Fig 1 (bottom) shows the phase composition and the evolution of heat flow of the cement paste containing 0.05 % of SP. At the beginning of hydration, ye'elimite is consumed as well as anhydrite, allowing ettringite and gypsum to immediately precipitate. With 0.05 % SP, gypsum is still detected until more than 3 hours of hydration even if it is quickly (less than half an hour) consumed in the reference. Also, anhydrite seems not to dissolve until there is no gypsum left in the cement; which is consistent with its slower dissolution.

Furthermore, ettringite precipitation is slower when SP is added, but the hydration scheme is similar: its precipitation is accelerated, which causes the second calorimetry peak. Then, its further acceleration in accordance with a faster ye'elimite dissolution causes the third stronger calorimetry peak. At 4 hours of hydration, the amounts of ettringite, ye'elimite and ferrite are in the same order of magnitude whatever the SP content.

As for AFm, it is detected earlier in presence of SP (from 1.5 h of hydration instead of 2.5 h), but in very low amount, suggesting local low concentrations of sulfate. Also, there is no significant evolution of AFm quantity until 4 hours of hydration, whereas it precipitates continuously at the beginning of the third peak of hydration in the cement without SP.

Concomitant dissolution of gypsum and ye'elimite, as well as ettringite precipitation acceleration are clearly linked. Therefore, SP must act either to a retardation of dissolution of the anhydrous species or to a prohibition of the hydrates nucleation and/or growth [40]; and when its effect is stopped, all hydration reactions directly continue.

3.1.3 Ettringite morphology

SEM micrographs of ettringite crystals formed in the cement paste with and without SP are presented on the Fig. 3 after 5 hours of hydration.

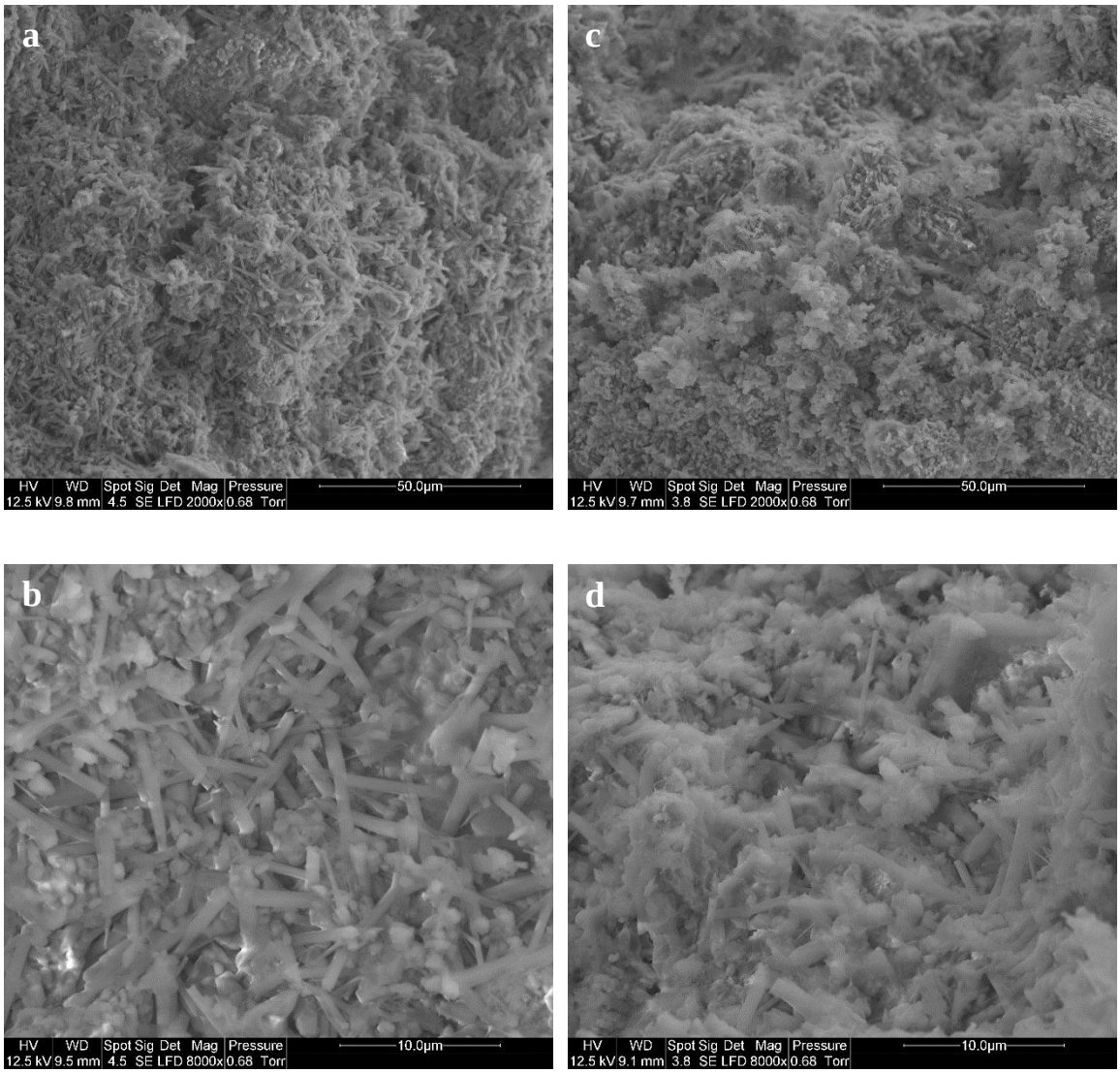

Fig. 3: SEM micrographs of fractured surfaces of BYF cement paste hydrated for 5 hours (a, b) without SP and (c, d) with 0.05 %SP

In cement paste with superplasticizer, heterogeneous sizes of ettringite crystals can be observed with the higher magnification (Fig. 3d); all of them seeming at first sight shorter or equivalent to the reference sample, even though one of the two ends of the

254 crystals is usually difficult to determine. Moreover, their diameters seem very
255 heterogeneous, from less than 0.1 µm to 1 µm. With the smaller magnification (Fig. 3c),
256 ettringite crystals are more difficult to recognize. Generally, it shows that ettringite
257 crystals are globally smaller when SP is added, suggesting a strong effect of SP on
258 ettringite precipitation. Previous studies on model systems [36,41] showed that
259 superplasticizers can inhibit crystal growth and therefore favor its nucleation; leading to
260 smaller crystals in a higher amount.

261 **3.1.4 Adsorption of the SP**

262 The amount of consumed SP was determined by subtracting the amount of remaining
263 superplasticizer in solution after centrifugation from the total amount of SP added to the
264 sample (depletion method [39]). The consumption isotherm of the SP at 40 min of
265 hydration is presented in Fig 4. The isotherm shows a high surface interaction between
266 SP and cement particles, which increases with the amount of SP added to cement. For
267 example, nearly 90 % of the SP added is consumed by the particles for cement paste
268 with 0.015 % SP. The isotherm starts to flatten out but does not reach a plateau with the
269 studied dosages. As shown in Fig 4, a continuous consumption of SP with increasing its
270 dosage is observed. This might be due to co-precipitation with the hydrates [42,43]
271 and/or the increase of available surface due to formation of small ettringite particles. It
272 is generally admitted that the presence of SP around the particles leads to electrosteric
273 repulsion, therefore the high adsorption of SP suggests a high potential of dispersion;
274 this will be discussed below, in the part 3.1.5 Rheological measurements.

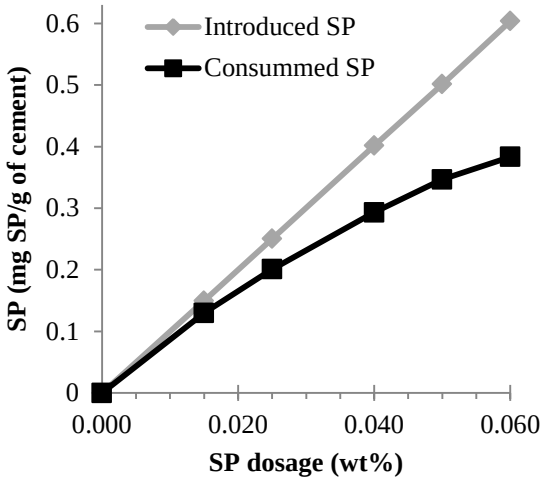

Fig 4: Consumption isotherm of the SP at 40 min of hydration

On the other hand, since the consumption rate concomitantly with the delay of hydration increase with the amount of SP added to the cement paste, it is expected that these two behaviors are linked.

Indeed, Plank and Hirsch showed that polycarboxylate superplasticizers have a preferential adsorption onto ettringite [33]. The effect of SP on ettringite morphology earlier described suggests the affinity between SP and ettringite. It can be speculated that when the solution is oversaturated with ettringite, nuclei form but don't grow because of SP adsorption onto them; the solution stays oversaturated so no further dissolution in ye'elimite, anhydrite nor gypsum can continue, which would explain the retardation of the hydration.

3.1.5 Rheological measurements

Yield stress corresponds to the minimum stress required to initiate flow. Depending on the measurement method, different types of yield stress can be defined. The yield stress determined by extrapolating the equilibrium flow curve to very low shear rates using rheological models is commonly termed dynamic yield stress. As reported by Roussel [44], yield stress is a relevant parameter able to describe the effect of superplasticizer on

the fluidity of cement pastes. Yield stress and viscosity at 100 s^{-1} of the cement paste with different additions of SP are presented in Fig 5. All measurements were made after 40 min of cement hydration, during the period of low activity. Indeed, it was pointed out by several authors that the fluidity of CSA pastes mostly depends on the amount of ettringite formed [30–32,45]. At the early stage of the hydration, it was previously shown that ettringite immediately precipitates, so the measurements were done during the low activity period, at a hydration time when the ettringite content was shown constant by *in situ* XRD. When increasing the amount of SP, the viscosity and shear stress decreases almost linearly. The shear stress almost reaches a zero-value when 0.06 % SP is added, while still showing a shear-thinning behavior. This shows that SP has a good dispersive action. Moreover, Su et al. [30] showed that fluidity is conserved as long as the ettringite amount is stable. The results of *in situ* XRD (Fig 1) showed that the precipitation of ettringite is delayed by the presence of SP; the fluidity can therefore be maintained longer with the use of SP.

The dispersive effect and rheological behavior of cementitious materials are closely related to the adsorption amount of SP onto the surface of cement particles. The optimum dispersion is reached when the total surface of cement particles is covered by superplasticizer (at the plateau) or sometimes before the plateau in the adsorption isotherm [46]. In fact, the electro-steric effect which controls the dispersive action depends on the surface coverage and the conformation of polymer [47]. At the saturation dosage (plateau), this effect only depends on the conformation of the polymer [47,48]. The minimum yield stress is generally reached after the plateau [49]. The adsorption isotherm presented in Fig 4 shows a beginning of a plateau at a dosage of 0.06%. At this dosage, cement paste displays a very low yield stress, which means that the saturation dosage could be close to 0.06%.

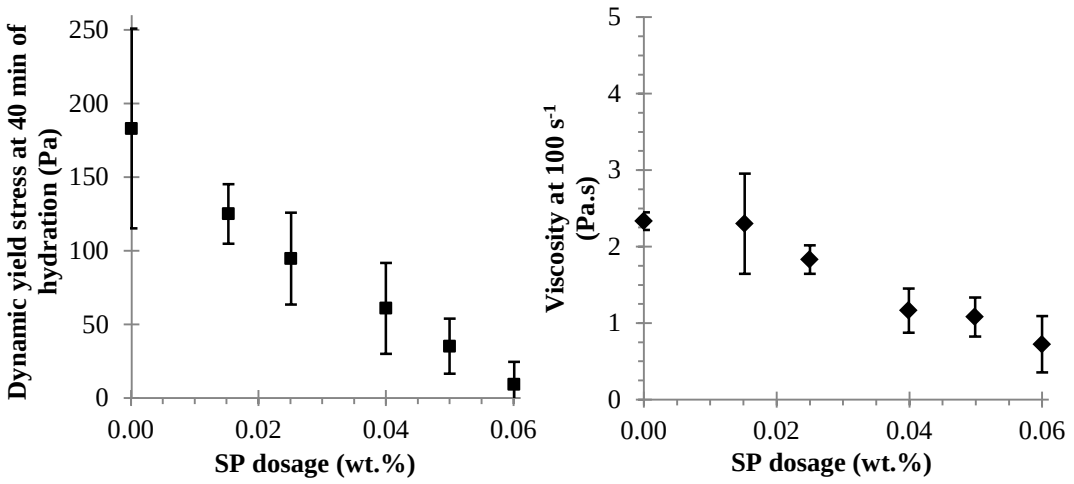

Fig 5: Effect of different amounts of the SP on rheological properties of cement paste at 40 minutes of hydration: a) shear stress and b) viscosity

3.2 SP effect at later ages

3.2.1 Phase composition

XRD results are shown in Fig 6. Due to the diversity of the AFm phases and the width of the resulting peak, the authors were not able to obtain a satisfying Rietveld refinement; consequently, the results were treated qualitatively.

In accordance with the previous results on hydration during the first hours and reactions (1) and (2), it shows that at 1 day of hydration, whatever the SP content, ye'elimite and anhydrite have reacted to form ettringite, monosulfoaluminate and aluminum hydroxide. Indeed, aluminum hydroxide is amorphous to X rays, but its presence is detected by TGA (not shown) with the weight losses after 230 °C [5,17,50,51]. Without SP (Fig 6), monosulfoaluminate continues to form while the amount of anhydrite decreases until 28 days of hydration. The first hydration product of belite is strätlingite (reaction (3)), it is first detected at 28 days of hydration. At this time, some ferrite has dissolved, this phase is suspected to be a source of iron and aluminum resulting in both formations of AFm and strätlingite [11]. At 90 days, katoite starts to precipitate, showing a partial

destabilization of strätlingite according to (4). At 6 months of hydration, the belite and ferrite contents are lower, showing a stronger reactivity of the two phases. XRD peak at 18° and weight losses at 450 °C indicate the presence of portlandite, which forms in the same time as C-S-H gel according to (5). The presence of amorphous hydration products is consistent with the relatively low amounts of strätlingite and katoite and high reactivity rates of belite and ferrite.

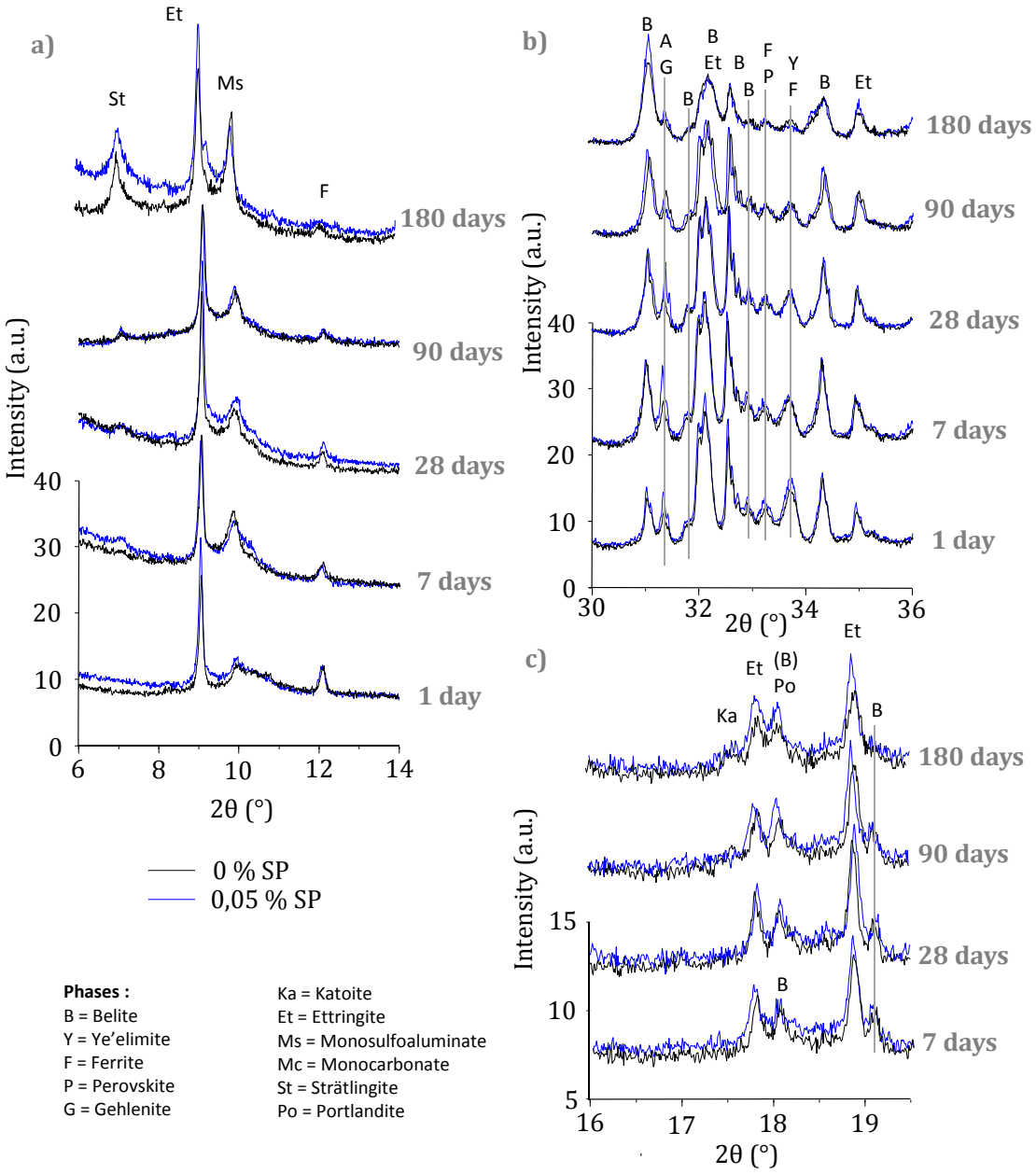

Fig 6: XRD patterns of cement without and with SP during its long-term hydration

With the addition of 0.05 % SP, during the first day of hydration fewer amounts of ettringite and calcium monosulfoaluminate have precipitated, according to both TGA and XRD results. This is linked with the retarding effect of SP. Monosulfoaluminate content increases until 7 days. At this time, some strätlingite precipitation is observed, way earlier than in the cement without SP. At 28 days of hydration the amount of strätlingite seems the same whatever the SP content, but the sample with SP has dissolved more belite and ferrite than the reference. A few portlandite precipitated, earlier than in the reference. Until 6 months of hydration, the amount of portlandite, strätlingite and katoite increases, in accordance with the decrease of belite, ferrite and aluminum hydroxide content. At 6 months, XRD pattern are almost stackable, showing a similar state of hydration.

As a conclusion on the effect of SP on the late age hydration, it can be pointed out that it diminishes the hydration rate of ye'elimite and anhydrite, but belite and ferrite react faster. Indeed, both strätlingite and portlandite were detected at earlier times when SP is added to the BYF cement paste; also, the hydration rate of belite and ferrite seems greater with SP from 7 to 90 days. However, at 6 months of hydration, both samples show the same phase assemblage.

3.2.2 Compressive strength

The compressive strength of the cement pastes at 1 day, 7 days, 90 days and 6 months are shown in the Fig 7. At one day of hydration, the compressive strength of the cement without SP is a bit higher than with increasing its amount. This is consistent with the calorimetry results, which show that at very short term, the SP has a retarding effect on the cement paste; and that this delay in the formation of the hydrates affects the

properties of the paste at least on the first day of hydration. For the next 90 days of hydration, no significant evolution in the compressive strength is observed, suggesting a very slow rate of hydration of the cement. Moreover, during this period, no significant effect of the SP on the compressive strength was neither observed; this consistent with a previous study [52]. Garcia Maté et al. [51] also tested the effect of a superplasticizer on the compressive strength of a CSA cement at young age (3, 7 days of hydration), and showed that it causes a slight increase or decrease, depending on the amount of calcium sulfate, which confirms that the effect of the superplasticizer on the compressive strength depends on the early age reactivity. It has to be noted that even if the hydration rate is slightly better in the presence of SP, the resulting compressive strengths are almost equivalent.

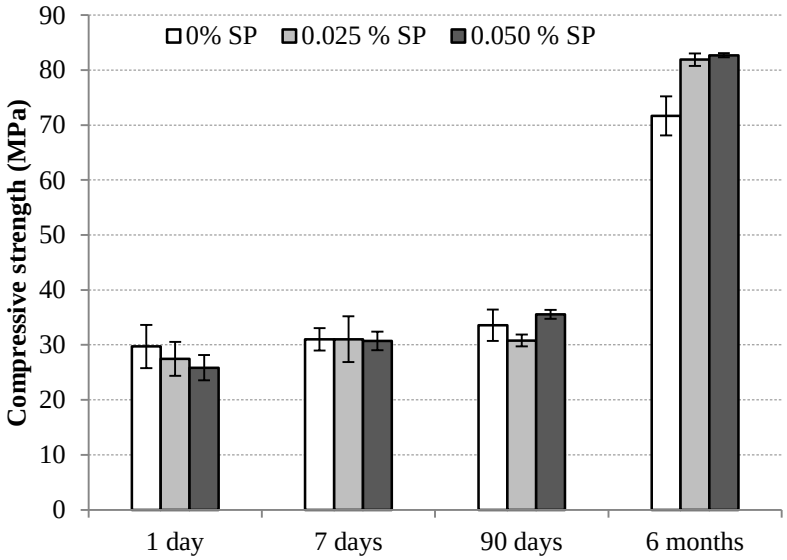

Fig 7: Compressive strength of cement paste containing different dosage of SP at different times of hydration

Nevertheless, between 90 days and 6 months of hydration, the compressive strength strongly increases; the increase is higher than the double of the 90 days value, suggesting a high reaction rate. The XRD data showed a strong activity in belite

hydration between those two hydration dates, suggesting the importance of the formation of a C-S-H in the strength of the paste. Moreover, at 6 months, the two samples containing SP show a compressive strength slightly higher than the ones without SP.

4 Conclusions

A polycarboxylate superplasticizer was shown to be compatible with the BYF cement paste for low dosages (below 0.06 %). Its effect on the hydration of a BYF cement paste was investigated both during the early and the later age. At short term, it was shown that SP has a retarding effect on the hydration, which increases with the SP dosage. The retard in hydration was related to the high adsorption capacity of the superplasticizer on the cement particles, and particularly, its interaction with ettringite results in its precipitation delay and a considerable change of morphology. Moreover, SP improves the rheological properties of the paste by decreasing both yield stress and viscosity; therefore a better workability is expected. In addition, the compressive strength is decreased during the first week due to the hydration delay. However, the delay is caught up at 7 days of hydration, and the strength is equivalent whatever the SP dosage until 90 days. During this period the cement hydration activity is very low. Nevertheless, after belite begins to react (between 3 and 6 months), the compressive strength strongly increases.

Acknowledgements

This work was financed by ED SCB and IMT Mines Alès. The authors wish to acknowledge LafargeHolcim for providing the cementitious materials and BASF for providing the polycarboxylate superplasticizer. Also, Romain Ravel and Arnaud

Regazzi are acknowledged for the 3D-printing of the molds used for *in situ* XRD and compressive strength samples, and Jean-Claude Roux for the SEM observations.

References

[1] J.G.J. (PBL) Olivier, G. (EC-J. Janssens-Maenhout, M. (EC-J. Muntean, J.A.H.W. (PBL) Peters, Trends in Global CO2 Emissions: 2016 Report, PBL Netherlands Environ. Assess. Agency Eur. Comm. Jt. Res. Cent. (2016) 86.

[2] E. Gartner, T. Sui, Alternative cement clinkers, Cem. Concr. Res. (2017). doi:10.1016/j.cemconres.2017.02.002.

[3] J.H. Sharp, C.D. Lawrencef, R. Yang, Calcium sulfoaluminate cements — low-energy cements , special cements or what?, Adv. Cem. Res. 11 (1999) 3–13. doi:10.1680/adcr.1999.11.1.3.

[4] K. Quillin, A. Dunster, C. Tipple, G. Walenta, E. Gartner, B. Albert, Project AETHER Testing the durability of a lower-CO2 alternative to Portland cement, in: 34th Annu. Cem. Concr. Sci. Conf., 2014.

[5] F. Winnefeld, S. Barlag, Calorimetric and thermogravimetric study on the influence of calcium sulfate on the hydration of ye'elimite, J. Therm. Anal. Calorim. 101 (2010) 949–957. doi:10.1007/s10973-009-0582-6.

[6] M. Ben Haha, F. Winnefeld, A. Pisch, Advances in understanding ye'elimite-rich cements, Cem. Concr. Res. 123 (2019) 105778. doi:10.1016/j.cemconres.2019.105778.

[7] A. Cuesta, G. Álvarez-Pinazo, S.G. Sanfélix, I. Peral, M.A.G. Aranda, A.G. De La Torre, Hydration mechanisms of two polymorphs of synthetic ye'elimite,

Cem. Concr. Res. 63 (2014) 127–136. doi:10.1016/j.cemconres.2014.05.010.

[8] G. Álvarez-Pinazo, A. Cuesta, M. García-Maté, I. Santacruz, E.R. Losilla, S.G. Sanfélix, F. Fauth, M.A.G. Aranda, A.G. De La Torre, In-situ early-age hydration study of sulfobelite cements by synchrotron powder diffraction, Cem. Concr. Res. 56 (2014) 12–19. doi:10.1016/j.cemconres.2013.10.009.

[9] V. Morin, G. Walenta, E. Gartner, P. Termkhajornkit, I. Baco, J.M. Casabonne, Hydration of a Belite-Calcium Sulfoaluminate-Ferrite cement : Aether TM, in: 13th Int. Congr. Chem. Cem., 2011: pp. 1–7. doi:10.1057/9780230616608.

[10] G.S. Li, G. Walenta, E.M. Gartner, Formation and Hydration of Low-CO 2 Cements Based on Belite, Calcium Sulfoaluminate and Calcium Aluminoferrite, 12th Int. Congr. Chem. Cem. (2007).

[11] J. Wang, Hydration mechanism of cements based on low-CO2 clinkers containing belite, ye'elimite and calcium alumino-ferrite, Université Lille 1, 2010.

[12] V. Morin, P. Termkhajornkit, B. Huet, G. Pham, Impact of quantity of anhydrite, water to binder ratio, fineness on kinetics and phase assemblage of belite-ye'elimite-ferrite cement, Cem. Concr. Res. 99 (2017) 8–17. doi:10.1016/j.cemconres.2017.04.014.

[13] E. Schmitt, Approche performantielle et microstructurale de la durabilité de bétons à base de ciments sulfoalumineux-bélitiques ferriques, Université de la Rochelle, 2014.

[14] G.Y. KOGA, Corrosion de renfort en acier noyé dans les matrices de ciment sulfoalumineux bélitique en fonction de l'hydratation, Université de Grenoble

Alpes, 2017.

[15] F. Winnefeld, B. Lothenbach, Phase equilibria in the system Ca 4 Al 6 O 12 SO 4–Ca 2 SiO 4–CaSO 4–H 2 O referring to the hydration of calcium sulfoaluminate cements, RILEM Tech. Lett. 1 (2016) 10–16.

[16] G. Álvarez-Pinazo, I. Santacruz, M.A.G. Aranda, Á.G. De la Torre, Hydration of belite–ye'elimite–ferrite cements with different calcium sulfate sources, Adv. Cem. Res. 28 (2016) 529–543. doi:10.1680/jadcr.16.00030.

[17] G. Álvarez-Pinazo, I. Santacruz, L. León-Reina, M.A.G. Aranda, A.G. De la Torre, Hydration Reactions and Mechanical Strength Developments of Iron-Rich Sulfobelite Eco-cements, Ind. Eng. Chem. Res. 52 (2013) 16606–16614. doi:10.1021/ie402484e.

[18] M. Fukuhara, S. Goto, K. Asaga, M. Daimon, R. Kondo, Mechanisms and kinetics of C4AF hydration with gypsum, Cem. Concr. Res. 11 (1981) 407–414. doi:10.1016/0008-8846(81)90112-5.

[19] G. Möschner, B. Lothenbach, F. Winnefeld, A. Ulrich, R. Figi, R. Kretzschmar, Solid solution between Al-ettringite and Fe-ettringite, Cem. Concr. Res. 39 (2009) 482–489. doi:10.1016/j.cemconres.2009.03.001.

[20] N. Meller, C. Hall, A.C. Jupe, S.L. Colston, S.D.M. Jacques, J. Phipps, The paste hydration of brownmillerite with and without gypsum : a time resolved synchrotron diffraction study at 30 , 70 , 100 and 150 u C, (2004).

[21] F. Winnefeld, S. Barlag, Influence of calcium sulfate and calcium hydroxide on the hydration of calcium sulfoaluminate clinker, ZKG Int. 12 (2009) 42–53.

[22] G. Azimi, V.G. Papangelakis, J.E. Dutrizac, Modelling of calcium sulphate

476 solubility in concentrated multi-component sulphate solutions, Fluid Phase
477 Equilib. 260 (2007) 300–315. doi:10.1016/j.fluid.2007.07.069.

478 [23] S. Allevi, M. Marchi, F. Scotti, S. Bertini, C. Cosentino, Hydration of calcium
479 sulphoaluminate clinker with additions of different calcium sulphate sources,
480 Mater. Struct. Constr. 49 (2016) 453–466. doi:10.1617/s11527-014-0510-5.

481 [24] I.A. Chen, M.C.G. Juenger, Synthesis and hydration of calcium sulfoaluminate-
482 belite cements with varied phase compositions, J. Mater. Sci. 46 (2011) 2568–
483 2577. doi:10.1007/s10853-010-5109-9.

484 [25] D. Jansen, A. Spies, J. Neubauer, D. Ectors, F. Goetz-Neunhoeffer, Studies on
485 the early hydration of two modifications of ye'elimite with gypsum, Cem. Concr.
486 Res. 91 (2017) 106–116. doi:10.1016/j.cemconres.2016.11.009.

487 [26] M. Zajac, J. Skocek, F. Bullerjahn, M. Ben Haha, Effect of retarders on the early
488 hydration of calcium-sulpho-aluminate (CSA) type cements, Cem. Concr. Res.
489 84 (2016) 62–75. doi:10.1016/j.cemconres.2016.02.014.

490 [27] F. Bullerjahn, M. Zajac, J. Skocek, M. Ben Haha, The role of boron during the
491 early hydration of belite ye'elimite ferrite cements, Constr. Build. Mater. 215
492 (2019) 252–263. doi:10.1016/j.conbuildmat.2019.04.176.

493 [28] L.E. Burris, K.E. Kurtis, Influence of set retarding admixtures on calcium
494 sulfoaluminate cement hydration and property development, Cem. Concr. Res.
495 104 (2018) 105–113. doi:10.1016/j.cemconres.2017.11.005.

496 [29] B. Ma, M. Ma, X. Shen, X. Li, X. Wu, Compatibility between a polycarboxylate
497 superplasticizer and the belite-rich sulfoaluminate cement: Setting time and the
498 hydration properties, Constr. Build. Mater. 51 (2014) 47–54.

doi:10.1016/j.conbuildmat.2013.10.028.

[30] T. Su, X. Kong, H. Tian, D. Wang, Effects of comb-like PCE and linear copolymers on workability and early hydration of a calcium sulfoaluminate belite cement, Cem. Concr. Res. 123 (2019) 105801. doi:10.1016/j.cemconres.2019.105801.

[31] W. Chang, H. Li, M. Wei, Z. Zhu, J. Zhang, M. Pei, Effects of polycarboxylic acid based superplasticiser on properties of sulphoaluminate cement, Mater. Res. Innov. 13 (2009) 7–10. doi:10.1179/143307509X402101.

[32] W. Guo, N. Sun, J. Qin, J. Zhang, M. Pei, Y. Wang, S. Wang, Synthesis and properties of an amphoteric polycarboxylic acid-based superplasticizer used in sulfoaluminate cement, J. Appl. Polym. Sci. 125 (2012) 283–290. doi:10.1002/app.35565.

[33] J. Plank, C. Hirsch, Impact of zeta potential of early cement hydration phases on superplasticizer adsorption, Cem. Concr. Res. 37 (2007) 537–542. doi:10.1016/j.cemconres.2007.01.007.

[34] N. Sun, W. Chang, L. Wang, J. Zhang, M. Pei, Effects of the chemical structure of polycarboxy-ether superplasticizer on its performance in sulphoaluminate cement, J. Dispers. Sci. Technol. 32 (2011) 795–798. doi:10.1080/01932691.2010.488132.

[35] M. Schönlein, J. Plank, Influence of PCE kind and dosage on ettringite crystallization performed under terrestrial and microgravity conditions, J. Am. Ceram. Soc. 101 (2018) 3575–3584. doi:10.1111/jace.15513.

[36] C. Shi, G. Zhang, T. He, Y. Li, Effects of superplasticizers on the stability and

morphology of ettringite, Constr. Build. Mater. 112 (2016) 261–266. doi:10.1016/j.conbuildmat.2016.02.198.

[37] D. Jansen, F. Goetz-Neunhoeffer, C. Stabler, J. Neubauer, A remastered external standard method applied to the quantification of early OPC hydration, Cem. Concr. Res. (2011). doi:10.1016/j.cemconres.2011.03.004.

[38] L. Pelletier-Chaignat, F. Winnefeld, B. Lothenbach, G. Le Saout, C.J. Müller, C. Famy, Influence of the calcium sulphate source on the hydration mechanism of Portland cement-calcium sulphoaluminate clinker-calcium sulphate binders, Cem. Concr. Compos. 33 (2011) 551–561. doi:10.1016/j.cemconcomp.2011.03.005.

[39] P. Déjardin, Volume effect of the adsorbed layer on the determination of adsorption isotherms of macromolecules by the depletion method, J. Phys. Chem. (1982). doi:10.1021/j100211a048.

[40] D. Marchon, R.J. Flatt, Impact of chemical admixtures on cement hydration, in: Sci. Technol. Concr. Admixtures, 2016. doi:10.1016/B978-0-08-100693-1.00012-6.

[41] A.M. Cody, H. Lee, R.D. Cody, P.G. Spry, The effects of chemical environment on the nucleation, growth, and stability of ettringite [Ca3Al(OH)6]2(SO4)3·26H2O, Cem. Concr. Res. 34 (2004) 869–881. doi:10.1016/j.cemconres.2003.10.023.

[42] F. Perche, Y.F. Houst, P. Bowen, H. Hofmann, Adsorption of lignosulfonates and polycarboxylates depletion and electroacoustic methods, in: 7th Int. Conf. Superplast. Other Chem. Admixtures Concr. Suppl. Pap., 2003: pp. 1–15.

[43] R. Flatt, I. Schober, Superplasticizers and the rheology of concrete, Woodhead Publishing Limited, 2011. doi:10.1016/B978-0-85709-028-7.50007-8.

[44] N. Roussel, Rheology of fresh concrete: From measurements to predictions of casting processes, Mater. Struct. Constr. 40 (2007) 1001–1012. doi:10.1617/s11527-007-9313-2.

[45] J.B. Champenois, C. Cau Dit Coumes, A. Poulesquen, P. Le Bescop, D. Damidot, Beneficial use of a cell coupling rheometry, conductimetry, and calorimetry to investigate the early age hydration of calcium sulfoaluminate cement, Rheol. Acta. 52 (2013) 177–187. doi:10.1007/s00397-013-0675-9.

[46] Y. Houst, R. Flatt, P. Bowen, H. Hofmann, U. Maeder, J. Widmer, U. Sulser, T. Buerge, Influence of Superplasticizer Adsorption on the Rheology of Cement Paste, (1999).

[47] R.J. Flatt, P. Bowen, Yodel: A yield stress model for suspensions, J. Am. Ceram. Soc. 89 (2006) 1244–1256. doi:10.1111/j.1551-2916.2005.00888.x.

[48] A. Perrot, T. Lecompte, H. Khelifi, C. Brumaud, J. Hot, N. Roussel, Yield stress and bleeding of fresh cement pastes, Cem. Concr. Res. 42 (2012) 937–944. doi:10.1016/j.cemconres.2012.03.015.

[49] C. Zhang, X. Kong, J. Yu, D. Jansen, J. Pakusch, S. Wang, Correlation between the adsorption behavior of colloidal polymer particles and the yield stress of fresh cement pastes, Cem. Concr. Res. 152 (2022). doi:10.1016/j.cemconres.2021.106668.

[50] K. Scrivener, R. Snellings, B. Lothenbach, A Practical Guide to Microstructural Analysis of Cementitious Materials, CRC Press, 2015. doi:10.1201/b19074.

[51] M. García-Maté, I. Santacruz, Á.G. De La Torre, L. León-Reina, M.A.G. Aranda, Rheological and hydration characterization of calcium sulfoaluminate cement pastes, Cem. Concr. Compos. 34 (2012) 684–691. doi:10.1016/j.cemconcomp.2012.01.008.

[52] X. Yuan, W. Chen, M. Yang, Effect of superplasticizers on the early age hydration of sulfoaluminate cement, J. Wuhan Univ. Technol. Mater. Sci. Ed. 29 (2014) 757–762. doi:10.1007/s11595-014-0992-6.

Appendix

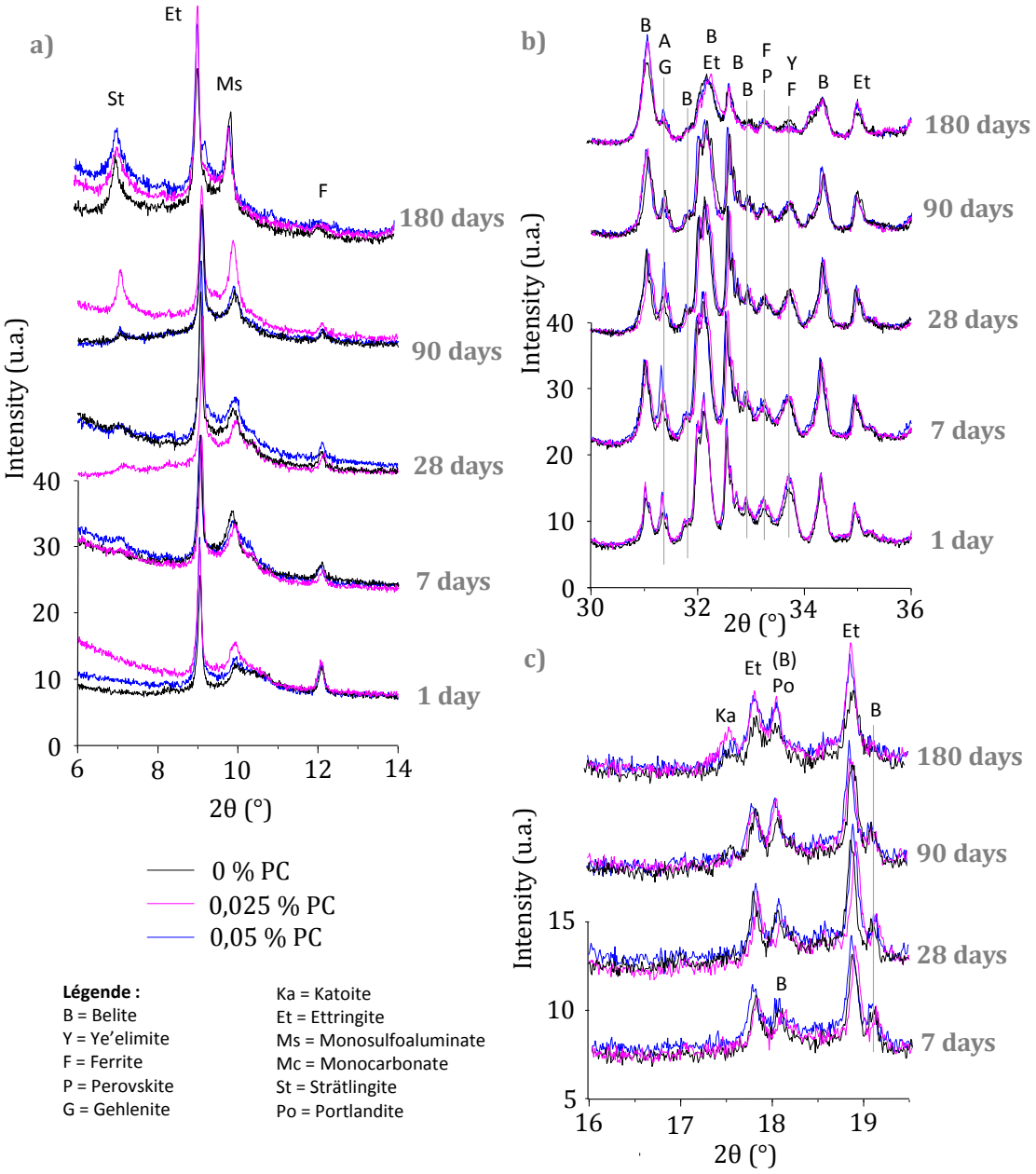

Fig. 1.A. XRD patterns of the hydrated cement pastes in the presence of polycarboxylate-based superplasticizer

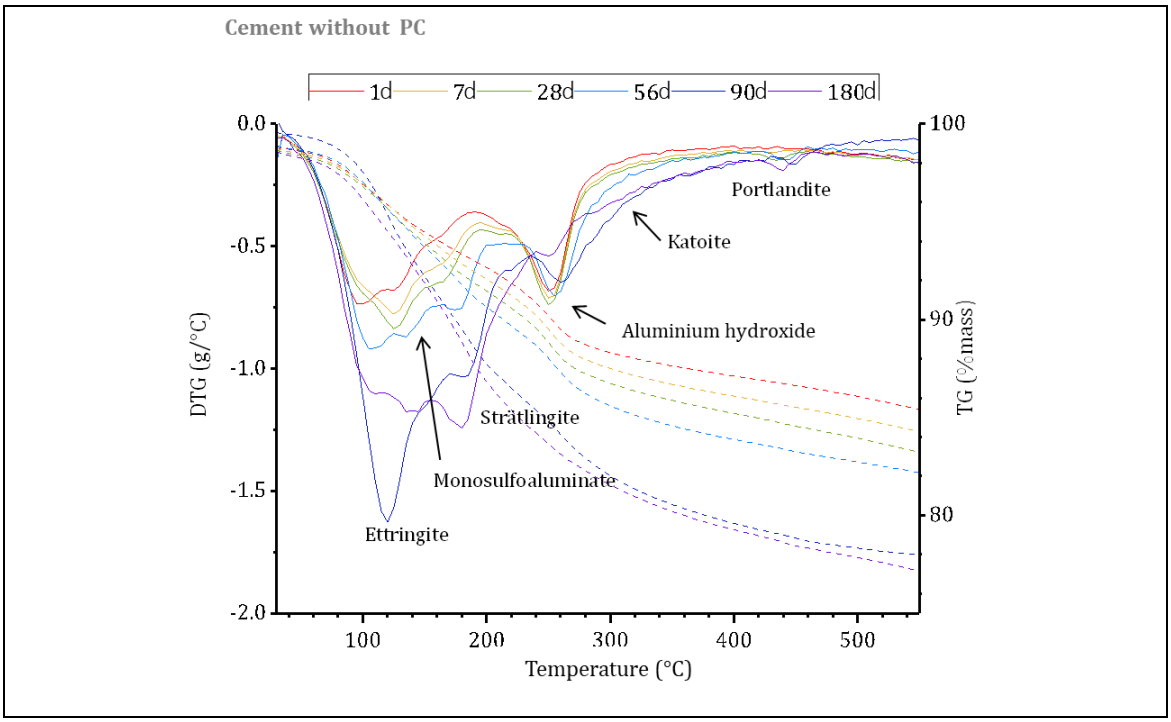
Cement without PC
1d
7d
28d
56d
90d
180d
0.0
-0.5
-1.0
-1.5
-2.0
DTG (g/°C)
100
90
80
TG (%mass)
100
200
300
400
500
Temperature (°C)
Portlandite
Katoite
Aluminium hydroxide
Strätlingite
Monosulfoaluminate
Ettringite

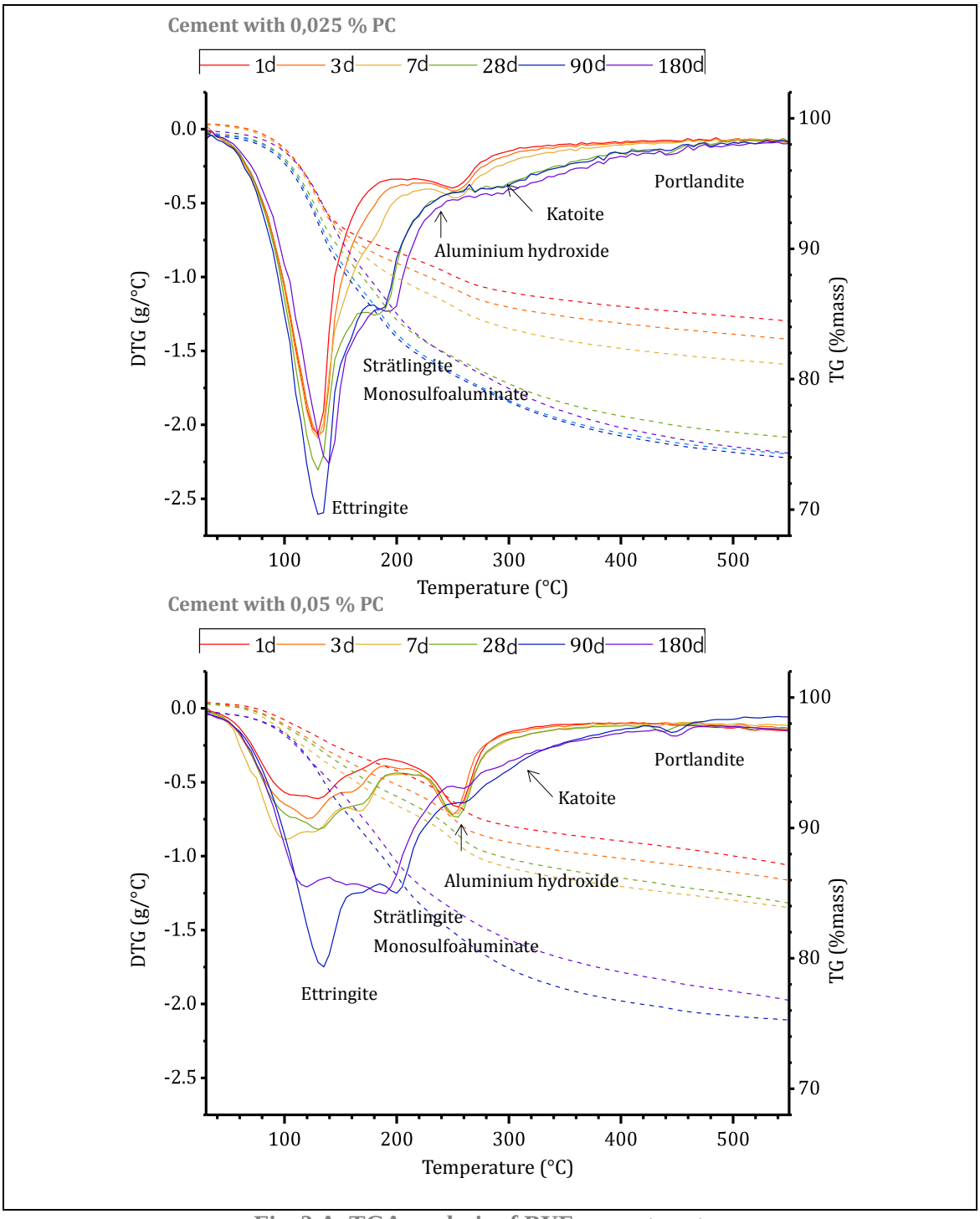

Fig. 2.A. TGA analysis of BYF cement pastes